RESEARCH ARTICLE

Structural resonance and mode of flutter of hummingbird tail feathers

Christopher J. Clark[1],[*], Damian O. Elias[2], Madeline B. Girard[2] and Richard O. Prum[1]

[1]Peabody Museum of Natural History, Yale University, PO Box 208106, New Haven, CT 06511, USA and [2]Department of Environmental Science, Policy and Management, University of California, Berkeley, 140 Mulford Hall, Berkeley, CA 94720, USA

[*]Author for correspondence at present address: Department of Biology, University of California, Riverside, CA 92521, USA (cclark@ucr.edu)

SUMMARY

Feathers can produce sound by fluttering in airflow. This flutter is hypothesized to be aeroelastic, arising from the coupling of aerodynamic forces to one or more of the feather's intrinsic structural resonance frequencies. We investigated how mode of flutter varied among a sample of hummingbird tail feathers tested in a wind tunnel. Feather vibration was measured directly at ~100 points across the surface of the feather with a scanning laser Doppler vibrometer (SLDV), as a function of airspeed, U_{air}. Most feathers exhibited multiple discrete modes of flutter, which we classified into types including tip, trailing vane and torsional modes. Vibratory behavior within a given mode was usually stable, but changes in independent variables such as airspeed or orientation sometimes caused feathers to abruptly 'jump' from one mode to another. We measured structural resonance frequencies and mode shapes directly by measuring the free response of 64 feathers stimulated with a shaker and recorded with the SLDV. As predicted by the aeroelastic flutter hypothesis, the mode shape (spatial distribution) of flutter corresponded to a bending or torsional structural resonance frequency of the feather. However, the match between structural resonance mode and flutter mode was better for tip or torsional mode shapes, and poorer for trailing vane modes. Often, the 3rd bending structural harmonic matched the expressed mode of flutter, rather than the fundamental. We conclude that flutter occurs when airflow excites one or more structural resonance frequencies of a feather, most akin to a vibrating violin string.

Key words: aeroacoustic, aeroelastic, scanning laser Doppler vibrometer, sonation, wind tunnel.

INTRODUCTION

Male hummingbirds in the 'bee' clade produce loud, species-specific sounds with their tail feathers during courtship displays (Clark et al., 2011b; Clark and Feo, 2008; Clark and Feo, 2010; Feo and Clark, 2010). In the companion paper (Clark et al., 2013), we provide evidence that the tail feathers of male hummingbirds produce these tonal sounds in high-speed airflow by aeroelastic flutter. Under this hypothesis, flutter of a feather is the result of feedback between aerodynamic forces on the feather and its internal structural (inertial/elastic) forces. Flutter is characterized by a critical velocity (U^*), below which flutter is damped, and above which damping is overcome and the feather exhibits a limit-cycle oscillation (Clark et al., 2013; Clark et al., 2011a). This onset of flutter is hypothesized to result from the physical coupling of aerodynamic forces to one or more of the feather's intrinsic resonance frequencies (Mandre and Mahadevan, 2010).

This hypothesis makes a key prediction that we test here: the mode of flutter at U^* is similar to an intrinsic resonance frequency of a feather in terms of both frequency and shape, where shape is the distribution of phase and amplitude of motion across the feather. These intrinsic resonance frequencies can be measured independently, such as by measuring a feather's free response to mechanical excitation. In flutter of airplane wings (i.e. at larger size scales), Bisplinghoff and colleagues (Bisplinghoff et al., 1996) suggested the vibration mode excited tends to be one of the lowest resonance modes, and may be either a torsional or bending mode. Other, more complex aspects of flutter, such as abrupt changes in mode shape or frequency of flutter, or multiple simultaneously

expressed modes of flutter, are allowed by the aeroelastic flutter hypothesis, as the coupling between aerodynamic forces and feather structure need not be linear. These behaviors are not predicted by the alternative hypothesis, in which flutter is vortex induced (Clark et al., 2013). Under this 'vortex whistle' hypothesis, mode of flutter is predicted to be transverse only (not torsional) and without complex spatial distribution.

Objects with complex 3D geometry, such as a feather, have a spectrum of normal modes of vibration, or resonance frequencies. Each individual resonance frequency has a unique mode shape, which is the spatial distribution across the object of relative phase and amplitude of oscillatory motion. These theoretical resonance frequencies are intrinsic, set by the geometric and material properties (mass and stiffness) of the object, along with its boundary conditions. When a load or an outside source of energy is applied (forcing) and the object vibrates in response, the frequency and distribution of the phase and amplitude of the object changes, for example due to deformation of the structure, or mode-locking (Fletcher and Rossing, 1998). The resulting observable oscillations are an 'operating deflection shape' (Richardson, 1997). Therefore, when air flows across a feather and causes it to flutter, the distribution of phase and amplitude of flutter across the feather is technically an operating deflection shape, which for simplicity we will hereafter call a 'mode of flutter'.

Here, we tested how the mode of flutter varies among hummingbird tail feathers tested in a wind tunnel (Clark et al., 2013), and how these modes of flutter compare with the structural resonance frequencies of these feathers. We quantified mode of flutter by

measuring the vibration of the feather directly with a scanning laser Doppler vibrometer (SLDV). This device shines a coherent laser on the surface of the feather and uses the Doppler shift of reflected light to calculate the instantaneous velocity in the direction parallel to the laser, across a series of points. SLDV does not require a reflectent to be applied to the surface, unlike regular LDV (Bostwick et al., 2010), allowing its use on objects as small as hummingbird feathers. We measured the feathers in the wind tunnel (see Clark et al., 2013), and also measured the resonance characteristics of a series of feathers stimulated across a range of frequencies by a shaker, an experimental paradigm in which the operating deflection shape approximates the normal modes. We also describe a related aspect of flutter with evolutionary significance: feathers may exhibit a dozen or more modes of flutter, and can abruptly switch or 'jump' from one mode of flutter to another.

MATERIALS AND METHODS

The wind tunnel, general methods and definitions for this experiment are as described in the companion paper (Clark et al., 2013). The feathers tested were from wild adult males of 14 species of 'bee' hummingbird (McGuire et al., 2009), obtained in the course of our fieldwork on each of these species under the relevant collecting and import permits. The exact feathers used and the species from which they were obtained are tabulated in the supplementary online material of our previous publications (Clark et al., 2011a; Clark et al., 2013). We tested the feathers in the wind tunnel in two ways. We performed qualitative experiments in which feather orientation [angles α and β – see fig. 2 in the companion paper (Clark et al., 2013)] were varied at a single airspeed (U_{air}), and we performed quantitative measurements of feather behavior at a constant orientation across a range of U_{air}.

Scanning laser Doppler vibrometry

Feathers were measured using an SLDV (PSV-I-400 LR, OFV-505 scan head, Polytec Inc., Irvine, CA, USA) fitted with a close-up attachment (PSV-A-410). This allowed a laser spot (~1 μm diameter) to be positioned with an accuracy of ~5 μm. A reference laser (PDV 100, Polytec Inc.) was pointed at the base of the feather, and remained stationary throughout the scans. Approximately 100 points were measured in a hexagonal grid fitted on each feather. Each point was scanned three times at a sampling frequency of 51.2 kHz for 0.64 s. While a scan was taking place, the feather was monitored to ensure that its acoustic behavior remained constant over time; scans in which the feather exhibited inconsistent behavior (i.e. varied with time) were re-run.

The maximum velocity the SLDV system could measure was $3 \, \text{m s}^{-1}$ and at higher U_{air} all feathers had individual points that greatly exceeded this maximum velocity. These points were not sampled. Similarly, some feathers had significant components of motion perpendicular to the laser that yielded points with spurious data. These points were identified manually and discarded. Calculation of average vibration power spectra at higher U_{air} only included regions of the feather that were below this maximum velocity. Hence, reported feather vibration amplitudes at these U_{air} underestimated the true average velocity amplitude of the entire feather.

Data from each scan were collected and analyzed in the program PSV 8.7 (Polytec Inc.). The PSV software computed an average spectrum for the entire feather allowing us to identify frequencies of maximum vibration. Mass-specific power spectral density (PSD) was calculated as acceleration^2 Hz^{-1}. Using relative phase data from the reference laser, we constructed animations of the mode of flutter

of each peak frequency identified from the PSD. These animations are presented as isolines, with normalized amplitude.

A change in U_{air} sometimes resulted in a small change in aeroelastic deformation, which then caused the feather to change its behavior, i.e. to change its mode of vibration, cause it to stop vibrating or exhibit 'inconsistent' behavior, in which it vibrated for a period, then abruptly stopped, then started again, etc. Each SLDV scan required 10–15 min to complete, and assumed time-invariant behavior. On rare occasions, if a feather was inconsistent and this prevented a scan from being run, it was rotated very slightly [Δα<2 deg; see fig. 2 of the companion paper (Clark et al., 2013)] to an orientation in which it produced sound consistently and the scan was rerun.

Mechanical stimulation experiments

To test their resonance properties, one to five individual feathers per feather type were affixed to a Brüel & Kjær mini-shaker 4810 (Naerum, Denmark) with hot melt adhesive at the calamus, and placed under the SLDV. The shaker was driven directly by the PSV software, which generated a frequency sweep from 0.01 to 15 kHz over the course of 0.640 s, to stimulate the feather. The physical displacement was <5 μm, significantly less than the thickness of the feather. These tests were run in still air, i.e. with possible added mass effects; this represents the natural condition, as the onset of flutter also occurs in air with possible added mass effects. Added mass estimates for the feathers were calculated assuming a cylinder of fluid around the feather (Blake, 1986) and are presented in supplementary material table S1 of the companion paper (Clark et al., 2013). The SLDV scanned ~300 points across the feather at a sampling rate of 51.2 kHz (fast Fourier transform, FFT: 12,800 lines, yielding a frequency resolution of 1.56 Hz). As a validation of the input signal, the PSV software calculated the coherence of the feather vibrations relative to the signal input to the shaker. Coherence was >0.5 (and usually >0.8) across the frequency range sampled, indicating that the shaker itself does not influence the results or conclusions presented here.

Average power spectra for all points across the feather were calculated. Amplitude maxima were interpreted to represent resonance frequencies, as there was no evidence of mode-locking or other effects that would cause the operating deflection shape to significantly depart from the structural resonance frequencies of the feather. Animations of the mode shape at the resonance frequencies were generated with the PSV software. These animations were compared with high-speed videos and SLDV scans of the feathers fluttering in the wind tunnel to identify modes similar to the modes of flutter exhibited in the wind tunnel.

The match between structural resonance frequencies and tip and torsional modes of flutter was strong, while the match for 'trailing vane' modes of flutter was somewhat poorer (see Results). One possible reason for this difference was our preparation of gluing the feather by the calamus, as we hypothesized that changes in this boundary condition could result in changes of some of the measured resonance frequencies of the feathers. Alternately, the scans of the entire feather sampled relatively few points on the trailing vane, so the resonance profile of this part of the feather may have been diluted by data from the other parts of the feather. To test these hypotheses, we conducted further tests on an additional five Costa's hummingbird (*Calypte costae*) R5, 10 Anna's hummingbird (*Calypte anna*) R5 and four Allen's hummingbird (*Selasphorus sasin*) R4, which are feathers with trailing vane modes in the wind tunnel. Using the SLDV we scanned 50–100 points in a linear transect that ran, midway down the feather, from the shaft to the

trailing vane. The feather was mounted two different ways, by the calamus (similar to previous trials) or with hot melt adhesive anchoring the leading vane and rachis, adjacent to the transect. Mounting location did not significantly affect the measured resonance frequency of the fundamental bending mode of the trailing vane (P=0.32, ANOVA with species and mounting type as factors) so replicate scans on the same feather were averaged for further statistical analyses, regardless of mounting type.

RESULTS

In general, all feathers tested in the wind tunnel were capable of fluttering and producing audible tones. Most of the feathers exhibited multiple modes of vibration under varying conditions. We investigated the modes of vibration as a function of shape, α, β and aeroelastic deformation qualitatively, and changes with respect to U_{air} quantitatively.

Modes of vibration: qualitative results

At moderately high U_{air}, rotating a feather through a range of α (e.g. ±90 deg) with β fixed revealed from one to ~10 discrete modes of flutter. Each mode had a unique shape and was excited at a specific frequency. We classified modes into types according to which region of the feather exhibited the greatest displacement; three commonly observed types are illustrated in Fig. 1A,B. 'Tip' modes were those in which the entire distal portion of the feather oscillated transversely, with a chordwise nodal line perpendicular to the shaft (Fig. 1C, nodal line lies between the red and blue isolines). Tip modes were often associated with pronounced aeroelastic deformation. Tip motion could also include significant torsion (twisting), and when the tip's motion was primarily torsional we term it a 'torsional' mode

with a nodal line parallel to flow (Fig. 1D), though these two categories were end-points on a continuum. 'Trailing vane' modes were those in which the trailing edge of the feather oscillated transversely, with a nodal line parallel to the feather's shaft (Fig. 1E). The 'dynamic bending mode' of white-bellied woodstar (*Chaetocercus mulsant*) R4 was unique and did not fit into the other categories (Clark et al., 2011a). Most feathers also exhibited 'whole-feather' modes, a bending mode that incorporated motion of the entire feather, typically at low frequency. Unlike tip, trailing vane and torsional modes, whole-feather modes were often influenced by attachment boundary conditions, i.e. the geometry of the insect pin holding the feather. Whole-feather modes also appear to be lab artifacts, and were not described in our previous publication (Clark et al., 2011a), as we have not identified any cases in which a whole-feather mode plausibly produces sound in an actual bird. We did not investigate them here for two reasons. First, in most cases whole-feather modes could only be elicited at extreme, unnatural angles that lacked biological relevance, such as negative values of β (i.e. the feather is pointing into the wind, which does not happen in typical bird flight). Second, whole-feather modes of flutter often caused the feather shaft to abruptly rupture.

For the feathers that exhibited multiple modes of vibration, most would express at least one trailing vane mode and one tip mode. These modes were usually observed in orientations similar to those the feather might have in a flying bird. Feathers held at a constant U_{air}, α and β mostly exhibited time-invariant vibratory behavior. Small changes to any of these variables sometimes caused a feather to abruptly shift its vibratory mode, which we call a 'mode jump'. Mode jumps were obvious when the feather jumped between mode types. For example, rotating an Anna's hummingbird R5 about β
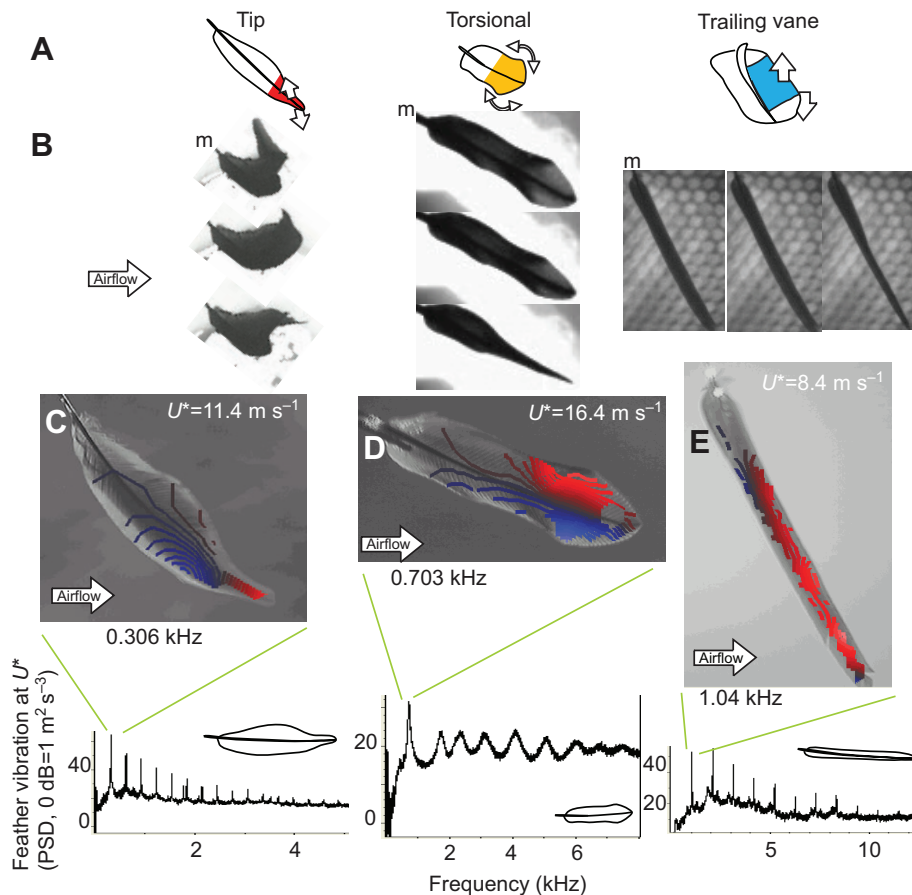

Fig. 1. Example of three types of mode of flutter: left, tip mode (broad-tailed hummingbird R2); center, torsional mode (Calliope hummingbird R1); and right, trailing vane (purple-throated woodstar R5). (A) Cartoons of the mode. (B) Three individual frames from high-speed videos taken at high airspeed ($U_{air}>U^*$), showing the extent of deformation possible. For source videos, see supplementary online movie of Clark et al. (Clark et al., 2011a). m indicates mounting location. (C–E, top panels) Fundamental frequency of mode of flutter as measured by the scanning laser Doppler vibrometer (SLDV) in the wind tunnel. Amplitude is depicted as isolines, and color indicates opposite phase. Spectra (bottom panels) are average power spectral density (PSD) from all points across the feather. Scans were taken at critical velocity (U^*), the lowest U_{air} at which flutter U_{air} was detected.
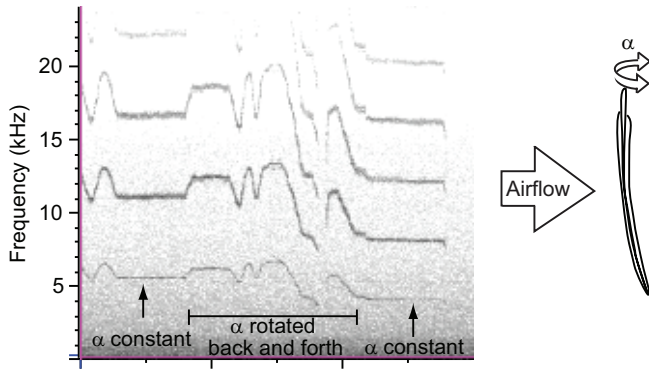
Fig. 2. Spectrogram of sound produced by white-bellied woodstar R4 in the wind tunnel as it is rotated back and forth about angle α. As feather orientation changed, sound frequency increased and decreased continuously, rather than jumping from mode to mode, as was observed in other feathers tested. U_{air}=21.2 m s^{-1}.

would cause it to jump from a trailing vane mode of ~3.5 Hz to a tip mode of ~1.2 kHz (similar to the effects of changing speed described below). Some feathers also had multiple modes of the same type that were often difficult to differentiate, especially multiple types of trailing vane modes. For instance, at a fixed U_{air} and β, rotating an Anna's hummingbird R5 through a small Δα might cause it to abruptly jump from 3 to 4 kHz mode, or rotating an Allen's hummingbird (_S. sasin_) R4 sometimes revealed both a 7 and a 9 kHz mode. In each case, high-speed video revealed only that the mode was a trailing-vane mode; high-speed video is poorly suited for mode

shape analysis, and the dropped points from the SLDV scans likewise limited their utility.

Mode jumps as a function of U_{air} are described further below. In addition to being caused by a change in boundary condition (i.e. changes in U_{air}, α or β), mode jumps occasionally occurred spontaneously. Sometimes these jumps were one way, i.e. a feather spontaneously jumped from mode A to mode B and thereafter exhibited only mode B, and sometimes the feather might jump back and forth between modes A and B, apparently at random. The same was true for the occasional feather that abruptly stopped fluttering, and then started again, etc. We term this time-varying behavior 'inconsistency'.

Although all feathers aeroelastically deformed in airflow, a subset of feathers seemed to exhibit especially pronounced bending, such as R2 and R3 of some _Selasphorus_ spp. and R4 of white-bellied woodstar (Fig. 2). Pronounced bending seemed to reduce the number modes a feather exhibited, and for these feathers we often only found one or two modes of vibration. Rotating such feathers through various α tended to not cause these feather to jump from mode to mode; rather, airflow-induced bending compensated for changes in orientation and resulted in a similar geometry of the tip of the feather, across a comparatively wide range of values of α and β.

Most feathers, when rotated through a wide range of angles at a given U_{air}, would change pitch. These changes in pitch were usually discontinuous, as a result of the feather jumping from one mode to another. A feather fluttering in one mode might vary in pitch slightly (<10%) with a small Δα, but rotating it through a large Δα would cause a mode jump, resulting in an abrupt change in pitch. One feather, white-bellied woodstar R4, was an exception: when rotated, this feather clearly varied continuously in its static deformation, and
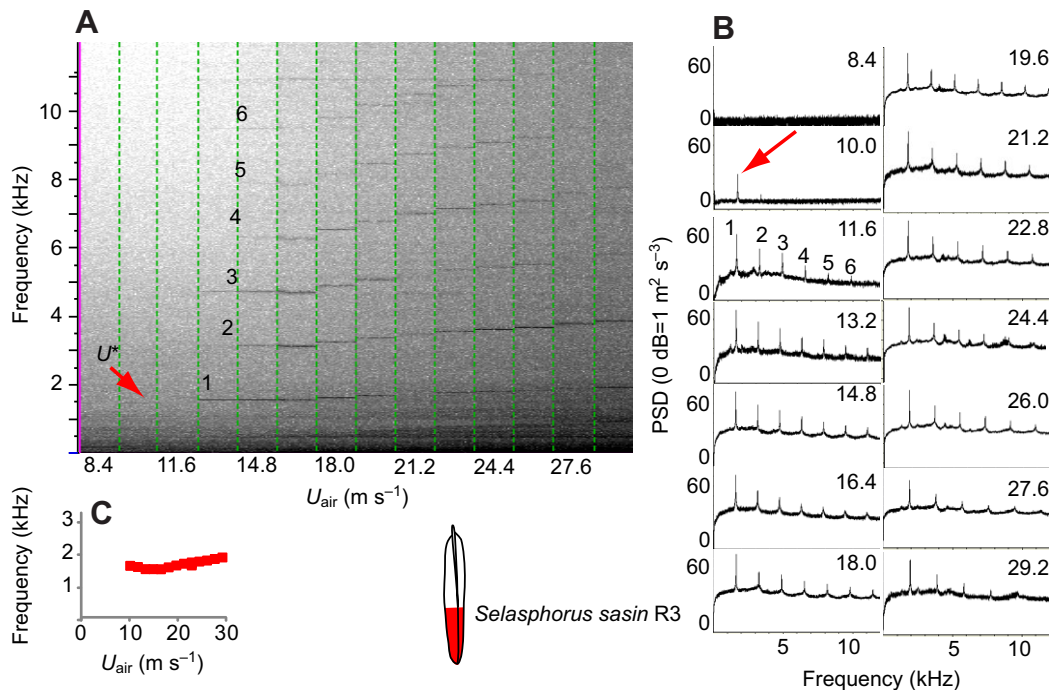

Fig. 3. Sound and vibration as a function of airspeed (U_{air}) of a feather that exhibited relatively simple behavior as a function of airspeed (compare with the complex behavior exhibited in Figs 4 and 5). (A) Sound spectrograms across a range of U_{air}. Individual spectrograms for each speed slice are separated by a green dashed line. Critical velocity (U^*) was 10 m s^{-1} (red arrow). Six harmonics are numbered, and vary in strength across U_{air}; the 2nd harmonic is dominant over the fundamental at some speeds >21 m s^{-1}. (B) PSD of vibration across the feather, from SLDV. U_{air} (m s^{-1}) is indicated in the top right of each spectrum. The red arrow corresponds to U^*. Six harmonics are present at most speeds, though bias in the SLDV data has altered the relative magnitude of the peaks. (C) Fundamental frequency as a function of U_{air}; these data are replotted in fig. 5 of the companion paper (Clark et al., 2013).
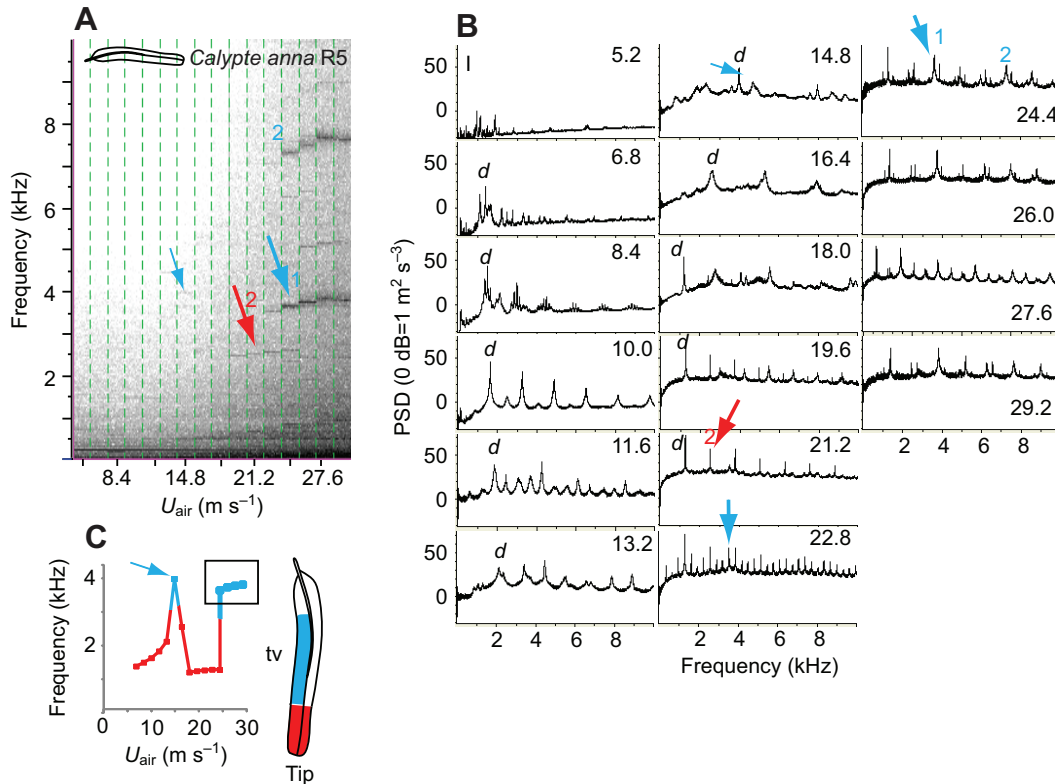
Fig. 4. Sound and vibration of an Anna's hummingbird R5 which exhibited three mode jumps across the range of U_{air} tested. Blue arrows indicate sound and vibration associated with the trailing vane of the feather, while red arrows indicate tip mode. (A) Sounds produced over a range of U_{air}; green lines separate spectrograms at each speed. In a mode jump at 22.8 m s^{-1}, the feather jumps from producing a 1.2 kHz sound with a tip mode (red arrow indicates 2nd harmonic; fundamental is not visible), to producing a ~3.5 kHz sound with the trailing vane (large blue arrow). An additional, brief mode jump occurs at 14.8 m s^{-1} (small blue arrow). (B) PSD of vibration across the feather, from SLDV. U_{air} (m s^{-1}) is indicated in the top right of each spectrum. The dominant vibratory frequency is labeled d and was omitted at the highest U_{air} because of bias in the SLDV data. Note that, above 22.8 m s^{-1}, the feather continued to vibrate at ~1.2 kHz (with little sound generated) as well as at ~4 kHz frequency, which produced significant sounds. (C) Sound and vibration fundamental frequency as a function of airspeed (U_{air}). tv, trailing vane. Owing to the mode jump, the data inside the box were plotted in fig. 5 of the companion paper (Clark et al., 2013).

simultaneously changed pitch continuously as a function of α [see also supplementary movie of Clark et al. (Clark et al., 2011a)]. As a result, at a constant U_{air} this feather could vary in pitch by up to 40% (Fig. 2).

Of the different modes of vibration that each feather exhibited, some were easier to elicit than others. Modes that corresponded to sounds that the birds produce during displays tended to be easiest to elicit. They also tended to produce the loudest sounds. Other modes were sometimes difficult to replicate, or were only produced under narrow ranges of U_{air}, α or β.

SLDV experiments at constant orientations

Twenty-seven types of feather taken from males of 14 species were tested with SLDV over a range of U_{air} to quantify the relationship between vibrations in the feathers and sound production. Each feather was measured at only one orientation.

Mode jumps as a function of U_{air} occurred in most of the feathers that were scanned. Mode jumps were obvious when the mode jumped was 'between-type', i.e. from a tip mode to trailing vane mode or *vice versa* (torsional modes were rare). These mode jumps could also be observed visually when the amplitude of vibration was high. Instances of abrupt, non-linear changes in flutter frequency also occurred in which we did not detect a change in the type of mode of flutter. High-speed videos suggested that these large

changes in frequency are mode jumps within a mode type, such as from one type of trailing vane mode to another.

We provide three in-depth examples that highlight notable aspects of flutter as a function of U_{air} (Figs 3–5). Fig. 3 provides an example of an Allen's hummingbird R4 that exhibited no mode jumps across the speed range tested, although non-linear behavior is still present as the 2nd harmonic becomes dominant at airspeeds above 22.8 m s^{-1} (Fig. 3A). In contrast, Fig. 4 provides an example of more complex behavior, an Anna's hummingbird R5 that underwent multiple between-type mode jumps. Fig. 5 shows an example in which, counter-intuitively, flutter frequency slightly decreased with U_{air} even if the two points below U^* are ignored (ordinary least squares regression, slope: −0.01, P=0.01).

These examples also show that individual feathers can flutter at multiple harmonically unrelated frequencies, simultaneously (Figs 4, 5). For example, the Anna's hummingbird R5 in Fig. 4B continued to inaudibly vibrate at ~1.2 kHz after the audible ~3.5 kHz mode was activated at U_{air}>22.8 m s^{-1}. An example of this is also present in Fig. 5, in which the purple-throated woodstar R5 fluttered and generated sound at ~0.9 kHz across the speed range tested (black arrows, Fig. 5A). Additional non-harmonic frequencies appeared in both the sound and vibration at some speeds (e.g. green arrows, Fig. 5A,B). Qualitative experiments in which purple-throated woodstar R5 were rotated about α at a constant U_{air} yielded modest
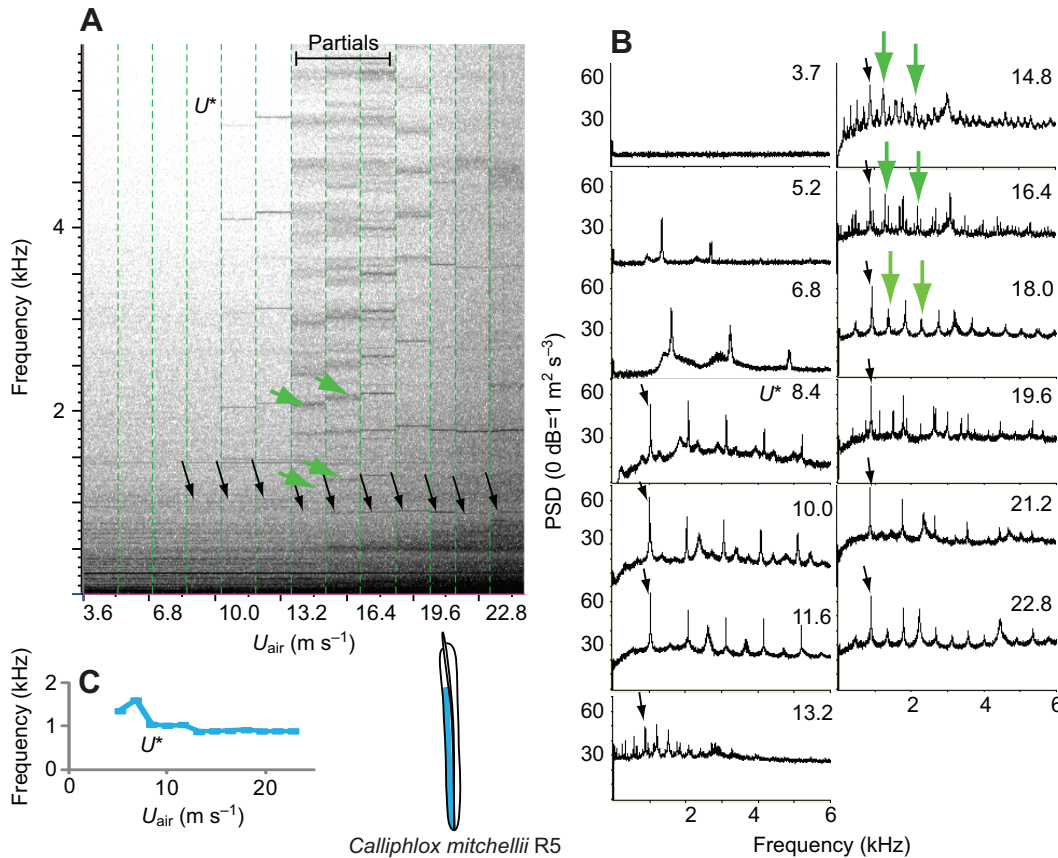
Fig. 5. Sound and vibration of a purple-throated woodstar R5 as a function of airspeed (U_{air}). Fundamental frequency did not increase with U_{air}. Non-integer harmonics, or 'partials', are produced at U_{air} 13.2–16.4 m s^{-1} (green arrows). (A) Sounds produced over a range of U_{air}. Black arrows indicate the fundamental frequency of sound; U^* indicates the onset of sound production. (B) SLDV vibration spectra corresponding to the sounds presented in A. Arrows correspond to those in A. Multiple additional vibratory peaks appear at non-integer frequencies. U_{air} (m s^{-1}) is indicated in the upper right of each spectrum. (C) Dominant frequency as a function of U_{air} [matching data are presented in fig. 5 of the companion paper (Clark et al., 2013)]. SLDV data suggest that the vibratory mode remains a trailing vane mode at all speeds, but the precise mode shape was unclear because of dropped points.

changes in frequency and similar changes in harmonic structure. We suspect that the appearance and disappearance of additional non-harmonic frequencies (Fig. 5), as well as the essentially flat relationship between frequency and U_{air}, are the result of small shifts in the mode shape of flutter, which were due to changes in feather aeroelastic deformation caused by changes in U_{air}.

Tests of feather structural resonance

Sixty-four feathers (of 23 rectrix types, one to five feathers per type) were scanned with SLDV as they were mechanically excited with a shaker, in order to measure their structural resonance. All feathers tested in this way exhibited multiple resonance frequencies. Added mass estimates for each feather are provided in supplementary material table S1 of the companion paper (Clark et al., 2013), and were lowest for feathers exhibiting trailing vane modes. In Fig. 6 we present examples of the resonance spectrum and six resonance frequencies for each of three feathers. The lowest resonance frequency corresponded to the first lengthwise bending mode of the entire feather (Fig. 6A,G,M) and varied from 0.089 to 0.82 kHz among the feathers tested. Most feathers exhibited additional lengthwise bending modes corresponding to odd integer harmonics (3rd, 5th,…) of the first mode, e.g. Fig. 6B,I,O, as expected for a bar clamped at one end and free at the other (Fletcher and Rossing, 1998). The higher harmonics of all feathers had spatially complex shapes that often involved motion of multiple feather regions (Fig. 6A–R).

We selected the resonance frequency from each scan that had the most similar mode shape to the mode of flutter of the feather at U^*. There was a strong correlation between the resonance frequency and the frequency of vibration at U^* in the wind tunnel (Fig. 7). Feathers exhibiting tip modes of flutter in the wind tunnel typically had a 3rd harmonic of the lengthwise bending mode at a similar frequency (i.e. the first permissible harmonic of a vibrating bar clamped at one end), in which a node was present at roughly 75% down the length of the feather (arrow in Fig. 6). Some feathers exhibited torsional resonance modes, particularly prominent in Calliope hummingbird rectrices (Fig. 7), which were the only feathers we tested that exhibited torsional modes of flutter in the wind tunnel.

In feathers that exhibited tip or torsional modes in the wind tunnel, the structural resonance frequencies were similar in shape to the flutter mode shape exhibited in the wind tunnel (Fig. 7). By contrast, trailing vane modes of flutter did not match as closely the shape of resonance modes measured by the shaker experiments (blue arrow in Fig. 7). In the wind tunnel, these feathers typically exhibited flutter in which the entire trailing vane oscillated with similar phase (i.e. in unison), without any localized nodes along the length of the trailing edge (Fig. 7, black arrow). None of the resonance frequencies revealed by the shaker experiments involved the entire trailing vane oscillating in phase; rather, all of the modes exhibited nodes that separated multiple regions of the trailing vane, which vibrated out of phase (e.g. Fig. 6P–R).

We hypothesized this mismatch between the mechanical stimulation experiments and those observed in the wind tunnel was due to our method of mounting or scanning the feather (see Materials and methods). Contrary to our hypothesis, additional scans of a transect of the trailing edge on Allen's R4, Costa's R5 and Anna's R5 yielded similar results to the whole-feather scans (Fig. 8). The transects revealed resonance frequencies that corresponded to fundamental and 3rd harmonic modes (Fig. 8B–E) within the trailing vane, but the resonance frequency of the fundamental was lower than the measured flutter frequency at U^* (Table 1) in all of the
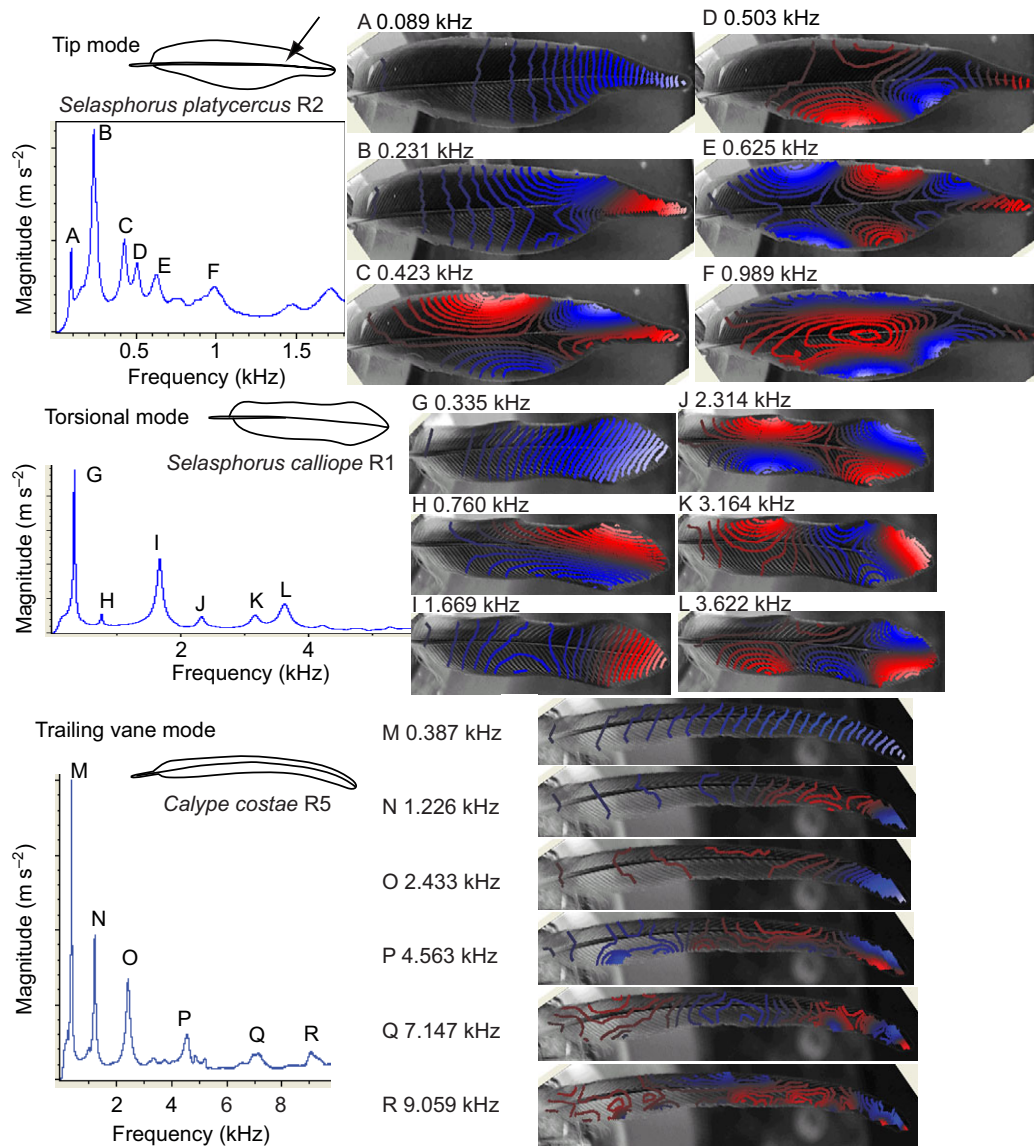
Fig. 6. Structural resonance frequencies of feathers exhibiting three different modes of flutter: broad-tailed hummingbird R2, tip mode (top), Calliope hummingbird R1, torsional mode (middle) and Costa's hummingbird, trailing vane mode (bottom), as stimulated by a shaker and measured by SLDV. The average response spectrum with the six highest response peaks (resonance frequencies) for each feather are indicated by uppercase letters. (A–R) Deflection isolines of the resonance frequencies, with darker lines occurring near the nodes (i.e. little displacement) and lighter lines nearer antinodes. Red *versus* blue indicates regions of opposite sign; isoline strength has been normalized within each panel (see response spectra peaks, left, for relative strength). A, G and M correspond to the fundamental longitudinal mode; B, I and O correspond to the 3rd longitudinal harmonic. H corresponds to a torsional mode. The remaining panels (C–F,J–L,N,Q,R) depict more complex resonance frequencies.

scanned feathers. Additional resonance frequencies were present in some of the scans that were close to the frequency at U^*, such as peak D in Fig. 8. The presence of multiple peaks corresponding to fundamental bending modes (Fig. 8C,D) appeared to be caused by the complex geometry of the feathers.

DISCUSSION

Our results demonstrate that feathers fluttering in airflow act as complex oscillators with multiple possible modes of flutter. Each mode represents a stable state within a dynamical system driven by complex interactions between aerodynamic, inertial and elastic forces on a feather. The modes we studied were usually stable, some over a wide range of parameter space (e.g. a range of U_{air}), and this region of stability was bounded by thresholds. Crossing a threshold, such as by changing the feather's orientation, would result in a mode jump, in which the feather would, in less than a few milliseconds, switch from one stable state to another.

Our measurements of the structural resonance of the feathers support the aeroelastic flutter hypothesis. All of the feathers we tested had structural resonance frequencies similar both in frequency and mode shape to the mode of flutter exhibited at U^* (Figs 7, 8). The

match was better in feathers exhibiting tip and torsional modes of vibration (Fig. 7). For feathers exhibiting trailing vane modes of flutter, the resonance modes elicited on the shaker were a qualitative match to the modes elicited in the wind tunnel. In these feathers, the frequency of flutter at U^* was broadly similar to one or more resonance frequencies (Figs 7, 8). But the resonance modes elicited by the shaker all had nodes midway down the trailing vane, whereas the entire trailing vane fluttered in phase in the modes of flutter elicited in the wind tunnel (Fig. 7B). Furthermore, the frequency of the most-similar mode was off by as much as 50% (Table 1, Fig. 7).

We have three related observations that may explain why these structural resonance frequencies of trailing vane modes were only a qualitative match with the flutter at U^*. First, our wind tunnel experiments did not examine the exact onset of flutter, as we sampled at discrete intervals of U_{air} and the SLDV recorded steady-state conditions. The true onset of flutter was a dynamic event lasting (we guess) <10 ms, at a U_{air} slightly below our reported U^*. During this transient event, even if the mode of flutter was initially similar to a resonance mode, the operating deflection shape (i.e. what we have called a mode of flutter) may evolve rapidly away from the resonance mode shape, as flutter amplitude rises *via* dynamic
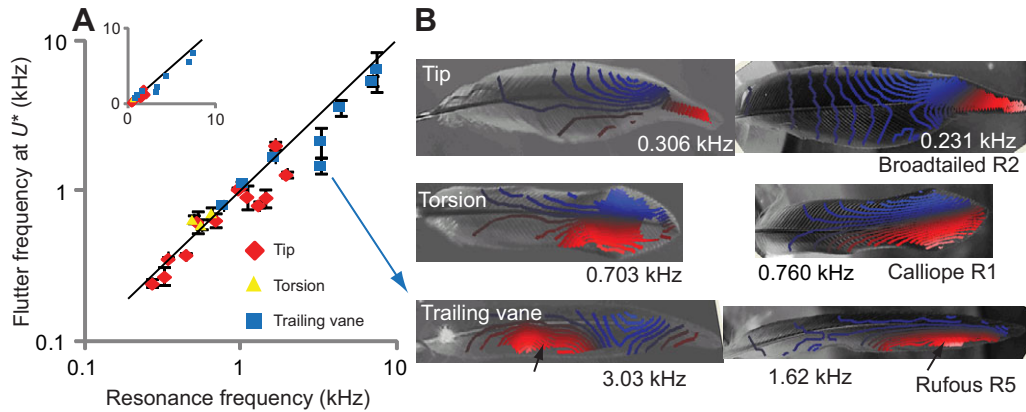
Fig. 7. (A) Mechanical resonance frequency (shaker stimulation) *versus* flutter frequency at $U*$ for 23 types of feather (N=1–5 feathers per type). Feathers exhibited multiple resonance frequencies (Fig. 6); resonance frequency plotted here was the mode with a shape most similar to the mode of flutter elicited in the wind tunnel. Bars indicate ± s.d. Black line indicates the 1:1 match predicted by the aeroelastic flutter hypothesis. Note the log axes; inset shows the same data on a linear scale. (B) Three examples of isolines of the fundamental frequency from flutter experiments (left) compared with isolines of a resonance frequency of the feather (right). Frequency and mode shape were more similar for tip (top) and torsional (middle) modes than they were for trailing vane modes (bottom). Different regions of the trailing vane exhibited maximal deflection in flutter *versus* resonance experiments (black arrows).

feedback. Second, the difference in mode shape between the shaker and wind tunnel may result from coupling between adjacent sections of the trailing vane (and/or the fluid in contact with this region) that, when stimulated by airflow, causes adjacent sections of trailing vane to flutter in synchrony. Third, the static aeroelastic deformation that all feathers exhibited in airflow may significantly modify the structural resonance frequencies in ways not replicated by the shaker experiments, in which the feathers were aerodynamically loaded by still, rather than moving, air.

Our original goal was to generate a model of flutter to predict what frequency of sound an untested feather would tend to produce. For example, consider an allometric argument: resonance modes of a beam scale $\propto L^{-2}$ and $\propto t$, where L is a characteristic length and t is thickness (Fletcher, 1992). If feather geometry scales isometrically ($L \propto t$), resonance frequency is expected to scale as L^{-1}. In support of this model, this allometric slope (-1) precisely fits the frequencies and lengths of the R5 of Anna's hummingbird, Costa's hummingbird and an Anna's×Costa's hybrid [see fig. 5C of Clark and Feo (Clark and Feo, 2010)] (see also Wells et al., 1978). However, generalizing this scaling relationship is difficult. The match in this specific instance appears to be caused by the close relationship of Anna's and Costa's hummingbirds, which are sister taxa. Each produces sounds with their outer tail feather (R5) *via* a similar trailing vane mode of flutter (Clark and Feo, 2010). We show here that individual feathers have many resonance frequencies (Fig. 6) and that the mode activated by flutter varies. Our *a priori* allometric prediction that *C. mulsant* R4 would produce sounds of roughly 13 kHz was off by an order of 2 (Fig. 2) because this feather does not exhibit a trailing vane mode; instead the mode of flutter it exhibited was novel. This allometric model also predicts that birds with much larger

feathers, such as vultures, ducks or hornbills should produce low-frequency flight sounds. Contrary to this hypothesis, many of the sounds these large-feathered taxa produce in flight are >1 kHz (C.J.C. and R.O.P., manuscript in preparation). This may be due to novel modes of flutter not observed in this sample of hummingbird feathers.

Individual feathers can express many modes of vibration, and we do not have a predictive model of which are more likely to be activated by airflow. We were surprised to find that 'tip' modes of flutter excited in the wind tunnel were typically the 3rd harmonic of the longitudinal resonance bending modes of the feather, rather than the fundamental (e.g. Fig. 6). Bisplinghoff and colleagues (Bisplinghoff et al., 1996) suggest that flutter in airplane wings is often the fundamental mode, which may correspond to destructive 'whole-feather' modes we avoided eliciting. And, although we found a structural resonance mode of Calliope hummingbird feathers that closely matched their predominant mode of torsional flutter (Fig. 6H), in the resonance spectrum, the magnitude of the torsional mode (peak H) is substantially lower than several others. Yet, it is easy to elicit torsional flutter in this feather, and we focused on this mode because this is the one expressed when this species makes sound with its tail (Clark, 2011). In conclusion, although we find support for the aeroelastic flutter hypothesis, it will need further refinement before general *a priori* predictions can be made of the sounds that a feather of given size and shape will make.

Implications for behavior

The data presented here, in combination with the data presented elsewhere (Clark et al., 2011a; Clark et al., 2013) have a number of implications for the ecology and evolution of aeroelastic flutter

Table 1. Structural resonance frequencies of the trailing vane, and the flutter frequency at $U*$

Species	Feather	Resonance fundamental frequency (kHz)	Resonance 3rd harmonic (kHz)	Flutter frequency at $U*$ (kHz)
Anna's hummingbird	R5 (10)	1.28±0.27[†††]	4.95±0.80	3.54±0.14 (2)
Costa's hummingbird	R5 (5)	3.66±1.10[††]	10.9±1.29	7.47 (1)
Allen's hummingbird	R4 (4)	3.78±0.46[†]	8.64±0.93	4.90±0.78 (2)

Sample size is given in parentheses. Resonance frequencies were measured *via* mechanical stimulation from a shaker, in still air.
Daggers indicate that the value differs from critical velocity ($U*$) flutter frequency (*t*-test), [†]$P<0.05$, [††]$P<0.005$, [†††]$P<0.001$.
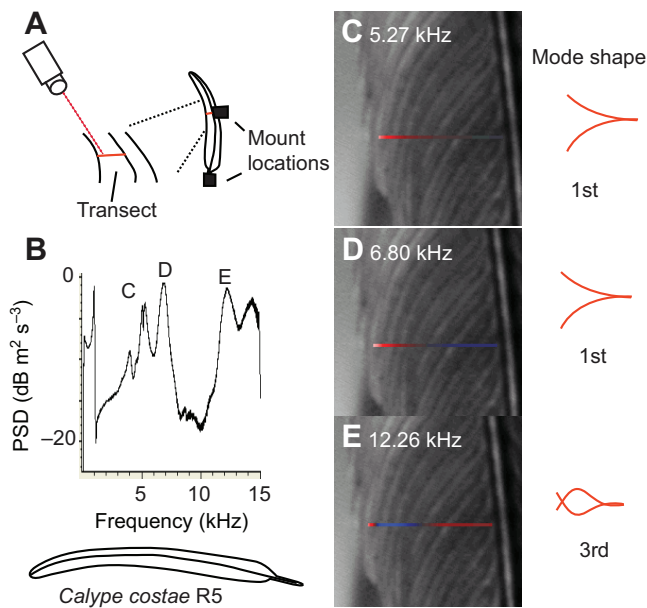
Fig. 8. Resonance frequencies of the trailing vane of a Costa's hummingbird R5. (A) SLDV scanned a transect from the rachis to the trailing vane of the feather. The feather was mounted either by the leading vane or by the calamus, and driven by a shaker (not shown). (B) PSD of all scan points from a transect. Peaks C and D correspond to fundamental transverse (bending) resonance frequencies, while peak E corresponds to the 3rd harmonic. (C–E) Mode shape along the transect for the labeled frequencies in B. See also Fig. 6 and Table 1.

of feathers, and the potential role of these sounds in avian communication. The sounds this sample of hummingbird feathers produced varied in frequency from ~0.3 to 10 kHz (Clark et al., 2013). Harmonic content likewise varied, from nearly pure tones (which sound similar to whistles) to buzzing sounds with dozens of harmonics, akin to the sound a bee makes in flight. In most feathers the sound was limited to discrete frequencies, set by the N modes of flutter the feather could exhibit, and by U_{air} (Clark et al., 2013), which is what we predict will be found in other birds that produce similar sounds. The white-bellied woodstar R4 is capable of pronounced frequency modulation as a function of feather orientation (Fig. 2). This feather appeared to be unique in this respect, and we do not expect pronounced frequency modulation to be common in the flutter-induced sounds of other birds.

All flight feathers that we tested could flutter and produce sound in the wind tunnel, regardless of whether that feather produces sound in flight (Clark et al., 2011a). Flutter is intrinsic to stiff, thin objects in fluid flow (Bisplinghoff et al., 1996), a description appropriate for all flight feathers. Therefore, all flying birds have the potential to contend with feather flutter as a passive byproduct of their flight (Clark et al., 2011a). Birds may be selected to avoid producing these sounds; three ways in which birds may avoid flutter are to fly at speeds below U^*, to avoid feather orientations at which flutter is promoted, or to hold the flight feathers so that the vanes of neighboring feathers overlap. Slotted wingtips and emarginated outer primaries decrease drag (Tucker, 1995), but as this orientation separates the vanes of neighboring feathers, we hypothesize it is prone to flutter and produce sound.

We argue that flight sounds likely arise initially as a passive, incidental byproduct of flight, but are then selected for a communication function (Clark et al., 2011a; Darwin, 1871; Prum,

1998). There are many examples of sounds produced during flight that are consistent with flutter, including the so-called whistling of the flight of ducks (Bahr and Pye, 1985) and doves (Hingee and Magrath, 2009), winnowing of snipe (Bahr, 1907; Miskelly, 2005; Reddig, 1978) or wing whirring of *Tyrannus* flycatchers (Smith, 1966), to name but a few. Given that all flight feathers have the potential to flutter, we predict that communication *via* this mechanism of sound production has arisen multiple times.

Controlled production of novel flutter-induced communication sounds would first evolve through the manipulation of flight kinematics that produce the first sounds, and could then proceed through selection on the form of these sounds to evolve changes in feather morphology to produce different aeroelastic deformation, new modes of flutter, etc. Our experiments reveal ways that birds may behaviorally modulate the production of sonations (Bostwick and Prum, 2003). Birds have the behavioral capacity to modulate the U_{air} over a feather, such as by modifying flight (or dive) speed (e.g. Clark, 2009), or in the case of sounds produced by outer wing feathers, by modifying wingtip kinematics (Clark, 2008). Increasing U_{air} resulted in an increase in pitch in most (but not all) of the feathers (Fig. 6). Moreover, in many cases the relationship between frequency and U_{air} was sufficiently shallow that Doppler shift will have a greater influence on the frequency heard or recorded than will flight speed [e.g. online appendix A of Clark and Feo (Clark and Feo, 2010)].

Ornithologists have long noted feathers with shapes that appear evolved for sound production (Bahr, 1907; Darwin, 1871; Delacour and Amadon, 1973; Snow, 1982). The data presented here suggest some correlations between feather shape, stiffness and the mode of flutter exhibited. Feathers with stiff rachi tended to express trailing vane modes, particularly if the feather has a high aspect ratio. Such feathers can easily express tip (or torsional) modes as well, but this shape appears to facilitate the expression of trailing vane modes. By contrast, of the feathers tested here, those with less stiff rachises and emarginated or tapered tips tended to principally express tip modes. The slightly reduced stiffness of the rachis appears to facilitate aeroelastic deformation which, as described above, may counteract the effects of changes in feather orientation, and result in the feather expressing relatively few modes of flutter. An emarginated or tapered shape to the feather tip, however, is not strictly necessary for a tip mode to be expressed (Clark, 2008). This may explain the pattern noted by Mahler and Tubaro (Mahler and Tubaro, 2001), who found that distinctive, attenuated outer primaries in pigeons are not phylogenetically correlated with the presence/absence of tonal wing sounds. These authors therefore suggested that emarginated feathers are unassociated with the presence/absence of flight sounds. But the data presented here show that such shapes are not preconditions for flutter and the ensuing tonal flight sounds. Rather, evolving a tapered or emarginated shape may function to modify the mode of flutter or the resonance frequency of a feather, or facilitate separation of the feather's vane from neighboring feathers (Feo and Clark, 2010). This is consistent with Mahler and Tubaro's data (Mahler and Tubaro, 2001), but suggests that emargination can nevertheless play a role in the evolutionary modification of flight sounds.

Most of the feathers tested here were capable of exhibiting multiple modes of flutter, and changing an independent variable such as orientation could cause a feather to jump from one mode of vibration to another (Figs 4, 5). We propose a parallel between this behavior of individual feathers in a wind tunnel, and how these sounds are likely to evolve. In most cases, our field data suggest that birds utilize just one mode of flutter per feather to produce sound, but there are slight exceptions. Anna's hummingbird R5, for example, can flutter

via a tip mode at roughly 1.3 kHz (Fig. 4, red), as well as a trailing vane mode with a roughly 3.5 kHz fundamental (Fig. 4, blue). It is this trailing vane mode that produces the loud, distinctive chirp of their dive sound (Clark and Feo, 2008), but just after that sound, there is an additional, short burst of 1.3 kHz sound [see fig. 2A in Clark and Feo (Clark and Feo, 2008)] produced just as the tail is being shut, i.e. as R5 is changing orientation. We attribute this additional pulse of sound to the tip mode of R5. While this is the best example of a mode jump from our field data, a similar process must have happened multiple times in the evolutionary history of the bee hummingbirds, such as from tip modes to trailing vane modes (Clark et al., 2011a), given a single origin of tail-sound production in the ancestor of the bee hummingbird clade. Evolutionary transitions in feather morphology and sound production mechanism likely occurred through an acoustically polymorphic intermediate state such as that observed in Anna's hummingbird. We expect that mode jumps akin to those that we artificially induced in a wind tunnel here should occasionally be present in the flight sounds of wild birds.

Mechanical sounds and sonations offer the opportunity to examine the evolution and function of sound production. Much as footsteps are the inevitable byproduct of terrestrial locomotion, flight inherently produces sound. These mechanical sounds may then evolve into sonations (i.e. mechanical sounds with communicative function). In addition to the flutter-induced sounds investigated here, other mechanisms of sound production in birds include percussion (Bostwick and Prum, 2003) and stridulation (Bostwick et al., 2010; Bostwick and Prum, 2005). Sonations serve a range of acoustical functions that parallels vocalizations, including signaling alarm, as in pigeons (Hingee and Magrath, 2009), courtship, as in manakins, snipe or hummingbirds (Bahr, 1907; Barske et al., 2011; Sutton, 1981), or male–male territorial interactions, as in todies or broadbills (C.J.C. and R.O.P., personal observations). Although vocalizations comprise the majority of bird communication sounds, the syrinx can only be accessed through surgery and therefore some types of question are difficult to study. Feathers, in contrast, are easily accessible for field manipulations, and the sounds they produce can be elicited in a wind tunnel. Subtle manipulations of the sounds produced by wild birds appear to be possible, such as adding a slight amount of mass (to lower resonance frequency) or trimming away a small part of a feather (to increase resonance frequency). Such experiments may allow the pitch that a wild bird produces to be 'tuned' slightly, enabling elegant manipulative experiments in the field to test sound function.

LIST OF SYMBOLS AND ABBREVIATIONS

f	frequency
L	characteristic length (e.g. aerodynamic chord)
PSD	power spectral density, mass specific
R1–5	tail feathers (rectrices): R1, innermost; R5, outermost
SLDV	scanning laser Doppler vibrometer
t	feather vane thickness
U_{air}	airspeed
U^*	critical airspeed at which aerodynamic energy exceeds damping, and the feather enters limit-cycle flutter
α	angle of attack: angle of the feather relative to airflow, corresponding to rotation about the feather's longitudinal (Y)-axis.
β	sweep angle: angle of the feather relative to airflow, corresponding to rotation about the Z-axis, perpendicular to the plane of the feather vane

AUTHOR CONTRIBUTIONS

C.J.C. and R.O.P. initiated the study; C.J.C. collected and analyzed wind tunnel data while M.B.G. collected structural resonance data; D.O.E. provided SLDV; R.O.P. provided equipment and support; all authors contributed to writing the paper.

COMPETING INTERESTS

No competing interests declared.

REFERENCES

Bahr, P. H. (1907). On the 'bleating' or 'drumming' of the snipe (*Gallinago coelestis*). *J. Zool.* **Part 1**, 12-35.

Bahr, P. H. and Pye, J. D. (1985). Mechanical sounds. In *A Dictionary of Birds* (ed. B. Campbell and E. Lack). Vermillion, SD: Buteo Books.

Barske, J., Schlinger, B. A., Wikelski, M. and Fusani, L. (2011). Female choice for male motor skills. *Proc. Biol. Sci.* **278**, 3523-3528.

Bisplinghoff, R. L., Ashley, H. and Halfman, R. L. (1996). *Aeroelasticity*. Mineola, NY: Dover Publications.

Blake, W. K. (1986). *Mechanics of Flow-Induced Sound and Vibration*. Orlando, FL: Academic Press.

Bostwick, K. S. and Prum, R. O. (2003). High-speed video analysis of wing-snapping in two manakin clades (Pipridae: Aves). *J. Exp. Biol.* **206**, 3693-3706.

Bostwick, K. S. and Prum, R. O. (2005). Courting bird sings with stridulating wing feathers. *Science* **309**, 736.

Bostwick, K. S., Elias, D. O., Mason, A. C. and Montealegre-Z, F. (2010). Resonating feathers produce courtship song. *Proc. Biol. Sci.* **277**, 835-841.

Clark, C. J. (2008). Fluttering wing feathers produce the flight sounds of male streamertail hummingbirds. *Biol. Lett.* **4**, 341-344.

Clark, C. J. (2009). Courtship dives of Anna's hummingbird offer insights into flight performance limits. *Proc. Biol. Sci.* **276**, 3047-3052.

Clark, C. J. (2011). Wing, tail, and vocal contributions to the complex signals of a courting Calliope hummingbird. *Curr. Zool.* **57**, 187-196.

Clark, C. J. and Feo, T. J. (2008). The Anna's hummingbird chirps with its tail: a new mechanism of sonation in birds. *Proc. Biol. Sci.* **275**, 955-962.

Clark, C. J. and Feo, T. J. (2010). Why do *Calypte* hummingbirds 'sing' with both their tail and their syrinx? An apparent example of sexual sensory bias. *Am. Nat.* **175**, 27-37.

Clark, C. J., Elias, D. O. and Prum, R. O. (2011a). Aeroelastic flutter produces hummingbird feather songs. *Science* **333**, 1430-1433.

Clark, C. J., Feo, T. J. and Escalante, I. (2011b). Courtship displays and natural history of the scintillant (*Selasphorus scintilla*) and volcano (*S. flammula*) hummingbirds. *Wilson J. Ornithol.* **123**, 218-228.

Clark, C. J., Elias, D. O. and Prum, R. O. (2013). Hummingbird feather sounds are produced by aeroelastic flutter, not vortex-induced vibration. *J. Exp. Biol.* **216**, 3395-3403.

Darwin, C. (1871). *The Descent of Man, and Selection in Relation to Sex*. Princeton, NJ: Princeton University Press.

Delacour, J. and Amadon, D. (1973). *Curassows and Related Birds*. New York, NY: The American Museum of Natural History.

Feo, T. J. and Clark, C. J. (2010). The displays and sonations of the black-chinned hummingbird (Trochilidae: Archilochus alexandri). *Auk* **127**, 787-796.

Fletcher, N. H. (1992). *Acoustic Systems in Biology*. New York, NY: Oxford University Press.

Fletcher, N. H. and Rossing, T. D. (1998). *The Physics of Musical Instruments*. New York, NY: Springer-Verlag.

Hingee, M. and Magrath, R. D. (2009). Flights of fear: a mechanical wing whistle sounds the alarm in a flocking bird. *Proc. Biol. Sci.* **276**, 4173-4179.

Mahler, B. and Tubaro, P. L. (2001). Attenuated outer primaries in pigeons and doves: a comparative test fails to support the flight performance hypothesis. *Condor* **103**, 449-454.

Mandre, S. and Mahadevan, L. (2010). A generalized theory of viscous and inviscid flutter. *Proc. R. Soc. A* **466**, 141-156.

McGuire, J. A., Witt, C. C., Remsen, J. V., Dudley, R. and Altshuler, D. L. (2009). A higher-level taxonomy for hummingbirds. *J. Ornithol.* **150**, 155-165.

Miskelly, C. M. (2005). Evidence for 'hakawai' aerial displaying by Snares Island snipe (*Coenocorypha aucklandica huegeli*). *Notornis* **52**, 163-165.

Prum, R. O. (1998). Sexual selection and the evolution of mechanical sound production in manakins (Aves: Pipridae). *Anim. Behav.* **55**, 977-994.

Reddig, E. (1978). Der ausdrucksflug der Bekassine (*Capella gallinago gallinago*). *J. Ornithol.* **119**, 357-387.

Richardson, M. H. (1997). Is it a mode shape, or an operating deflection shape? *Sound and Vibration Magazine* 1-11.

Smith, W. J. (1966). Communication and relationships in the genus *Tyrannus*. *Publ. Nuttall Ornithol. Club* **6**, 1-250.

Snow, D. W. (1982). *The Cotingas*. London: British Museum.

Sutton, G. M. (1981). On aerial and ground displays of the world's snipes. *Wilson Bull.* **98**, 457-477.

Tucker, V. A. (1995). Drag reduction by wing tip slots in a gliding Harris' hawk, *Parabuteo unicinctus*. *J. Exp. Biol.* **198**, 775-781.

Wells, S., Bradley, R. and Baptista, L. F. (1978). Hybridization in *Calypte* hummingbirds. *Auk* **95**, 537-549.